공학석사학위논문

손끝 햅틱 장비를 위한 의사 햅틱의 활용

Cutaneous Fingertip Haptic Device with Pseudo-Haptics Effect

2016 년 2 월

서울대학교 대학원

기계항공공학부

장 인 영

Abstract

Cutaneous Fingertip Haptic Device with Pseudo-Haptics Effect

Inyoung Jang
Mechanical & Aerospace Engineering
The Graduate School
Seoul National University

We propose a novel design of cutaneous fingertip haptic device and approach of integrating pseudo-haptics into our cutaneous haptic device. With 2-DoF cutaneous device, angle-force calibration result is presented for its operation. Then, 3-DoF cutaneous haptic device is designed for more realistic contact feedback in virtual reality (VR). Prelimineary result of integrating cutaneous device and hand tracking device for complete wearable haptic interface is also demonstrated. Meanwhile, we explore possible utility of pseudo-haptics for cutaneous fingertip haptic device, whose performance is inherently limited due to the lack of kinesthetic feedback. We experimentally demonstrate that: 1) pseudo-haptics can render virtual stiffness to be more rigid or softer only by modulating visual cue; and 2) pseudo-haptics can be used to expand the range of the perceived virtual stiffness to be doubled.

Keywords: Cutaneous haptic feedback, Wearable haptic device, Pseudo-haptics, Fingertip Perception, Multimodal
Student Number: *2013-20710*

Contents

List of Figures **iv**

Abbreviations **vi**

Symbols **vii**

1 Introduction **1**

1.1 Motivation and Objectives 1

1.2 Related Works 3

2 Cutaneous Fingertip Haptic Device **6**

2.1 2-DoF Cutaneous Haptic Device 6

2.1.1 Design and Specification 6

2.1.2 Angle-Force Calibration 8

2.1.3 Application of 2-DoF Cutaneous Haptic Device 10

2.2 3-DoF Cutaneous Haptic Device 11

2.2.1 Design and Specification 11

2.2.2 Control Design 14

2.2.3 IMU Distortion Offset Calibration 17

2.2.4 Device Validation 20

2.2.5 Integration with Wearable Hand Tracking Interface 21

3 Pseudo-Haptics with Cutaneous Haptic Feedback **25**

3.1 Limitation of Cutaneous Haptic Device 25
3.2 Application of Pseudo-Haptics Effect 26

4 Experimental Study **28**
4.1 Experimental Settings 28
4.2 Experiment #1 32
4.3 Experiment #2 34
4.4 Experiment #3 36
4.5 Discussion 38

5 Conclusion and Future Work **40**
5.1 Conclusion 40
5.2 Future Work 41

List of Figures

2.1 2-DoF cutaneous fingertip haptic device using dual motors and encoders. 7
2.2 Dual motor 2-DoF cutaneous haptic device generating the normal and directional force. 7
2.3 Angle-force calibration result for 2-DoF cutaneous haptic device with humans as surrogate force sensor [1, 2]. 9
2.4 Multi-user haptic collaborative manipulation (above). Teleoperation simulation of ROV (below). 2-DoF cutaneous haptic devices are worn on the index finger and thumb to provide contact force feedback. 11
2.5 3-DoF cutaneous haptic device. 12
2.6 3-DoF cutaneous haptic device design. The device is composed of two main parts: body and contact plate, which are connected by three wires actuated by three motors. 12
2.7 3-DoF cutaneous haptic device scheme. 14
2.8 Result of magnetometer distortion calibration. When calibration applied to yaw rotation, RMS error of yaw angle decreased from 36.39° to 9.70° 18
2.9 IMU on cutaneous device distorted by motors' ferromagnetism (left). IMU distortion calibrated (right). 19
2.10 Step response of normal desired force for 3-DoF cutaneous haptic device. The dashed black line represents the reference force, and blue line represents the measured contact force from FSR sensor on contact plate. The rising time is about 0.2s. 20

2.11 Sinusoidal response of roll and pitch angle for 3-DoF cutaneous haptic device. The dashed black line represents the reference angle given by corresponding (directional) sinusoidal reference force. The blue line represents the rotation angle from IMU sensors attached to the device. 21
2.12 A 3-DoF cutaneous fingertip haptic device is integrated with our IMU-based hand tracking device. 6 IMU sensors of hand tracking device measure the rotations of finger segments for finger/hand localization. 22
2.13 Preliminary experiment of the integrated wearable haptic interface; hand tracking device can capture any hand posture, while contact haptic feedback is given by 3-DoF cutaneous haptic device. 24

3.1 Human perception rapidly deteriorates due to the lack of kinesthetic haptic feedback, when solely using cutaneous haptic device. 26

4.1 Environmental scene. 30
4.2 Virtual 3D environment with fingertip sphere, reference plane (RF-plane) without pseudo-haptics effect, and pseudo-haptics plane (PH-plane) with pseudo-haptics effect applied (right). 31
4.3 Result of Experiment #1: modulation of perceived virtual stiffness via pseudo-haptics effect α. 33
4.4 Result of Experiment #2: expansion of the renderable range of the perceived virtual stiffness via pseudo-haptics effect α. 35
4.5 Result of Experiment #3: confusion induced by contradictory haptic and visual cues. 37

Abbreviations

VR	**V**irtual **R**eality
DoF	**D**egree **o**f **F**reedom
FSR	**F**orce **S**ensitive **R**esistor
IMU	**I**nertial **M**easurement **U**nit
2AFC	**2**-**A**lternative **F**orced-**C**hoice

Symbols

$\{s_b\}$	Reference frame on device body	
$\{s_c\}$	Reference frame on contact plate	
f	Fingertip contact force in $\{s_b\}$	mN
f^d	Desired contact force in $\{s_b\}$	mN
a_i	Vertex position of body part in $\{s_b\}$	mm
b_i	Vertex position of contact plate part in $\{s_c\}$	mm
h	Geometric center position of contact plate in $\{s_b\}$	mm
R	Rotation matrix of $\{s_c\}$ w.r.t. $\{s_b\}$	$\in \Re^{3\times 3}$
α	A ratio of virtual displacement to real displacement	

Chapter 1

Introduction

1.1 Motivation and Objectives

Some brilliant advances in virtual reality (VR) technologies have been achieved recently. Wearable VR devices, including Oculus Rift® and Microsoft Hololens®, allow human users to experience an immersive virtual reality with 3D visual feedback. With the appearance of these devices, human user can now consider virtual reality as a significant world, where they have a chance of various indirect experiences with reality. Meanwhile, haptic feedback devices have received a lot of interest with the demand for more authentic sensation in virtual world, as haptic feedback handles a substantial amount of human perception as well as visual feedback.

However, conventional haptic devices including Force Dimension's Omega® and Geomagic's Omni® are not considered to be a suitable approach, in that these devices generally focus on displaying the kinesthetic haptic feedback, a sense of touch from musculoskeletal systems like bones, muscles, and tendons. Even though the kinesthetic devices can exert relatively large force feedback, they are usually bulky and mechanically grounded with limited workspace, which critically harm the wearability and portability of wearable VR devices. Instead, cutaneous haptic devices providing tactile sensation from finger skins can avoid those issues, which is expected to create a lot of synergy with wearable VR devices. Besides that, cutaneous devices display the contact perception of virtual world in the same way of sensing an object in real world, by dexterous hands.

While utilizing these cutaneous haptic devices in VR, the realism of the haptic sensation deteriorates during contact due to the lack of kinesthetic feedback, which is basically supposed to maintain the user's fingertip at the virtual object's boundary. In order to prevent this problem, cutaneous devices are commonly used together with kinesthetic devices. However, to maintain the advantage of solely using cutaneous haptic device, a concept of pseudo-haptics effect, an illusionary haptic feedback using visual cue modification, can be a possible solution. By using pseudo-haptic feedback, a fabricated haptic sensation can generated without any physical devices. We believe that this property of pseudo-haptics can be applied to cutaneous haptic devices to relieve its inherent limitation.

Our research objective in this thesis is to develop wearable cutaneous fingertip haptic device and to examine the possible application of integrating pseudo-haptics effect to our cutaneous haptic device. A novel design for cutaneous device is considered to present 2 and 3-DoF contact force onto user's fingertip. Then, experimental study of human perception is demonstrated to investigate the effectiveness of pseudo-haptics effect when combined with our cutaneous fingertip haptic device. As a first step, we consider the contact perception of normal plane with 2-DoF cutaneous haptic device in this thesis.

1.2 Related Works

First of all, the possibility of using cutaneous fingertip haptic feedback has been researched (e.g., [3]) with various designs for cutaneous fingertip haptic devices including [4–9]. Among these researches, a novel approach of using dual motors, from [4], enabled the utility of wearable cutaneous haptic device with 2-DoF contact force. Similar designs were applied and improved, followed by [1, 5, 6, 10–12]. This 2-DoF device design was also used in researches of haptic interface for remote users [5] and haptic telepresence system [12], while it seems to lack specific modeling or sensing contact force which is significant to provide proper force feedback. In order to display more realistic contact information, 3-DoF cutaneous haptic devices are also considered in [13–19]. Design of using voice coil actuator was applied in [13] to generate 3D contact feedback. A piezoresistive sensor and cable design was utilized in [14] with micro DC motors attached.

Some recent researches [16, 17] include the design of using rigid links, to avoid the uncertainty caused by cable design and compliant human fingertip. Some of these devices were combined with devices for finger/hand localization to present the complete wearable haptic interface [20–22], however, most of them utilized camera-based approach which can occur issues of occlusion.

While using these cutaneous haptic devices, limitation of using the devices *alone* was also noticed [1], where the penetration through virtual surface in VR harms user's sensation. Similar phenomenon noticed by [18, 23–26], a concept of sensory substitution was proposed, insisting some possibility of utilizing cutaneous haptic feedback without kinesthetic haptic feedback.

The concept of pseudo-haptic feedback to efficiently simulate haptic sensation includes the modification of perceived haptic properties such as mass [27], friction [28], stiffness [28, 29], and texture [30, 31]. Some applications of using this pseudo-haptics were investigated for simulating the perception of weight [32] and gripping force [33]. However, since most of the results were proceeded with passive haptic device or even without any physical device, users are deemed to perceive insufficient haptic perception. Regarding the interaction with virtual object's surface, enhancing haptic feedback for palpation in medical field using pseudo-haptics was examined in [34]. Integration of pseudo-haptics into vibrotactile device was also proposed in [35, 36], to display the sensation of virtual bump.

In this thesis, we propose 1) design of 2-DoF cutaneous device with angle-force calibration result, 2) design and control of 3-DoF cutaneous device using wire, IMU sensors, and 3) possible usage of pseudo-haptics effect integrated with cutaneous haptic device. We adopt the 2-DoF device design from [4], and develop angle-force calibration result [1, 2] in order to generate desired contact force onto user's fingertip, which is unclearly done in previous researches. A novel 3-DoF cutaneous haptic device is also proposed; three DC motors with wires connected to contact plate. IMU sensors are then calibrated to measure the rotation of contact plate, to display the desired 3D contact force. This IMU-based design also has possibility of integration with our IMU-based hand tracking device [37], where finger/hand localization is critical in wearable haptics. Experimental study for human perception using pseudo-haptics effect together with cutaneous device is also demonstrated. With limited device performance, we examine if pseudo-haptics can partially substitute the absence of kinesthetic feedback, which can be a pioneering approach. The rest of this thesis structured as follows. Sec. 2 contains the development of 2-DoF and 3-DoF cutaneous haptic devices [1, 2]. Sec. 3 presents an approach of applying pseudo-haptics to cutaneous haptic devices. Experiments for this application are given in Sec. 4, and concluding parts in Sec. 5.

Chapter 2

Cutaneous Fingertip Haptic Device

2.1 2-DoF Cutaneous Haptic Device

2.1.1 Design and Specification

Based on the design principle of [4, 5], 2-DoF cutaneous fingertip haptic device [1, 2] was constructed as shown in Fig. 2.1 and Fig. 2.2. The device is equipped with two motors (Maxon® DCX motor, $\phi = 10$mm, 3W, $16:1$ gear ratio), each of which has encoder with the resolution of 1024 cnt/rev attached to its motor shaft. Using USDigital® USB4 DAQ board and Arduino® UNO microcontroller

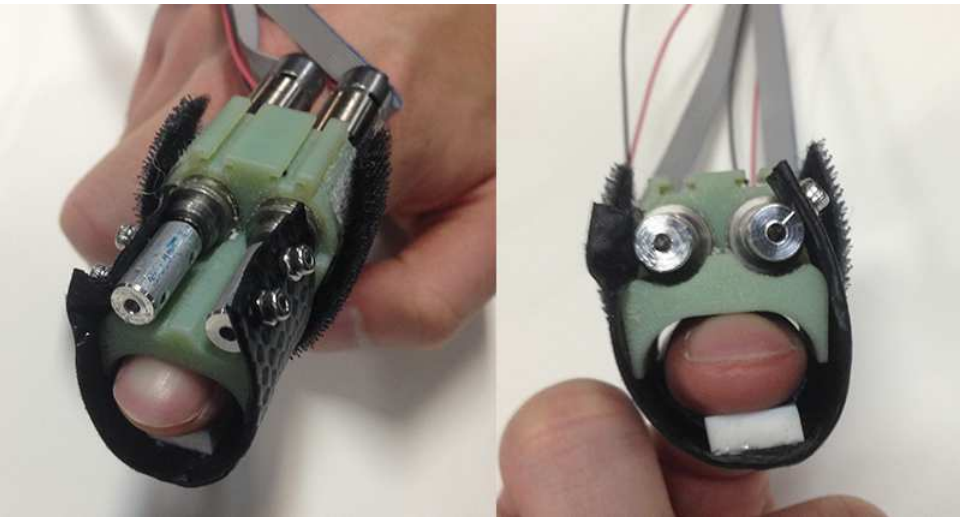

FIGURE 2.1: 2-DoF cutaneous fingertip haptic device using dual motors and encoders.

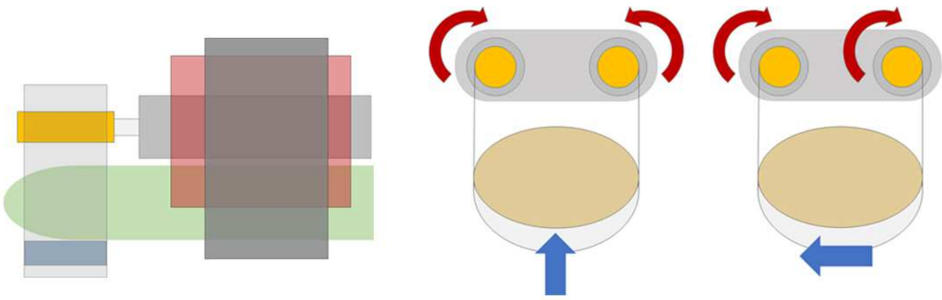

FIGURE 2.2: Dual motor 2-DoF cutaneous haptic device generating the normal and directional force.

board, current angle of motor is measured and controlled in about 1kHz. The rubber block is attached between the band and human finger in order to transmit the motor torque right onto the fingertip.

During haptic manipulation in virtual reality, 2-DoF contact force (i.e.; normal and shear force) is transmitted to user's fingertip via the device. The normal contact force to the user's fingertip is produced by rotating the two motors in the opposite direction, while the shear force produced in the same direction.

2.1.2 Angle-Force Calibration

Fingertip force of the device is then controlled by proper rotation of the motors. For this, calibration of the motors' rotation angle to the fingertip force is necessary. However, it is difficult to robustly measure a contact force of human fingertip, while its compositions, shapes, and compliances differ from each person. Instead, as introduced in [1, 2], the idea of utilizing human subject as a surrogate force sensor can be a possible solution. In other words, we used the calibration result based on the responses of human subjects.

In detail, we first set a certain maximum torque for the motor, which is limited by motor's specification or device design. It is then applied to the subject's fingertip and the motor rotation angle at that moment is measured. This is defined as the maximum rotation angle for 100% maximum force. The subject is then asked, while regulating the motor angle from zero to maximum, when he/she

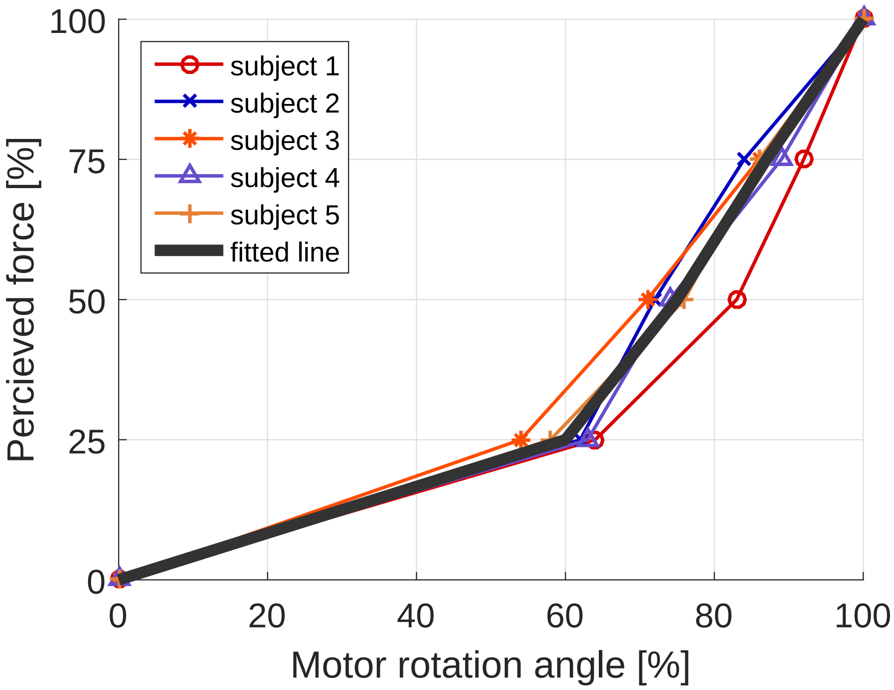

FIGURE 2.3: Angle-force calibration result for 2-DoF cutaneous haptic device with humans as surrogate force sensor [1, 2].

perceives the half of the maximum force, to set 50% spot of the maximum force. By repeating this process with the range of 0-50% and 50-100%, the angles for 25% and 75% of the maximum force are measured. Therefore, desired rotation angles for perceived 25%, 50%, 75% of the maximum torque are identified in each trial.

The calibration result is shown in Fig. 2.3, which demonstrates a consistent trend among five different subjects. Each subject carried out 5 trials of process above and average data were used after normalizing maximum angles to be 100. The graph suggests that it is possible to calibrate the angle-force relation of this device by a combination of two linear lines, with the breakaway point approximately at 60% of the maximum motor angle with 25% of the maximum motor torque. This calibration result between motor rotation angle and human-perceived force is utilized to produce a desired force for our 2-DoF cutaneous haptic device.

2.1.3 Application of 2-DoF Cutaneous Haptic Device

Worn on the fingers, this 2-DoF cutanoues haptic device is applicable to any haptic tasks in virtual reality. With the advantage of wearability and relatively less limited workspace, our device was utilized for various experiments and simulations of haptic experience in virtual reality. In Fig. 2.4, two human users haptically collaborate in virtual reality via internet as shown in FIG..., contacting with virtual objects (cube, cup, etc.) or moving those objects together. While interacting with objects, haptic feedback of contact or grasping is given to users' fingertip with the help of cutaneous devices worn on the index finger and thumb. Similar system was applied to the teleoperation simulation of remotely operated vehicle (ROV) in [38]. The human user perceives as if the ROV is user itself, while ROV manipulator is mapped to user's arm and hand. The gripping force is transmitted to user as the manipulator grasps the cylinders.

In various cases including both above, haptic feedback, especially cutaneous haptic feedback, can offer an immersive and realistic experience of virtual world with proper visual feedback.

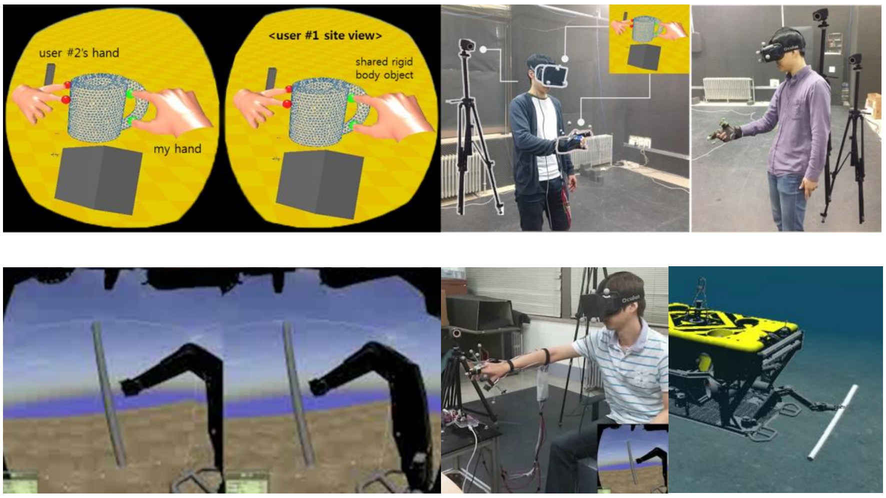

FIGURE 2.4: Multi-user haptic collaborative manipulation (above). Teleoperation simulation of ROV (below). 2-DoF cutaneous haptic devices are worn on the index finger and thumb to provide contact force feedback.

2.2 3-DoF Cutaneous Haptic Device

2.2.1 Design and Specification

For more realistic fingertip sensation, as in real world, we developed 3-DoF cutaneous haptic device in succession to 2-DoF device above. By enlarging degree of freedom of contact force provided by the cutaneous device, human user is

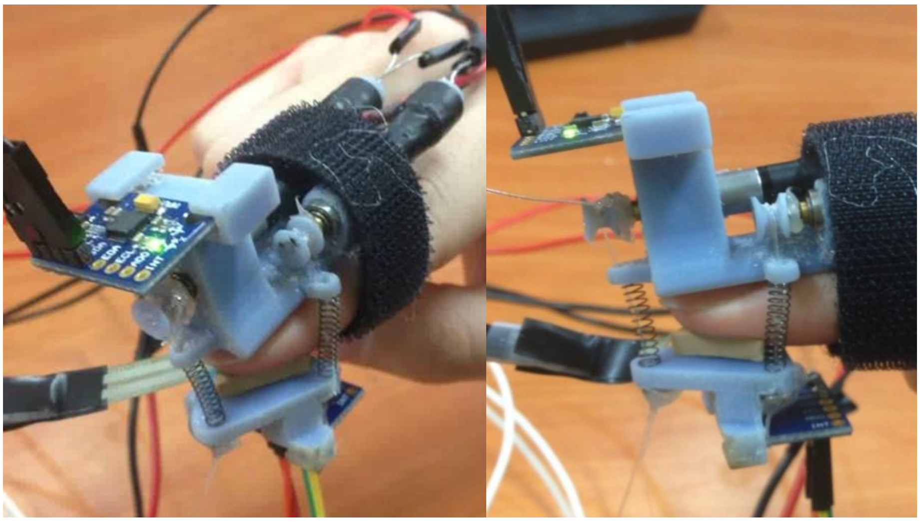

FIGURE 2.5: 3-DoF cutaneous haptic device.

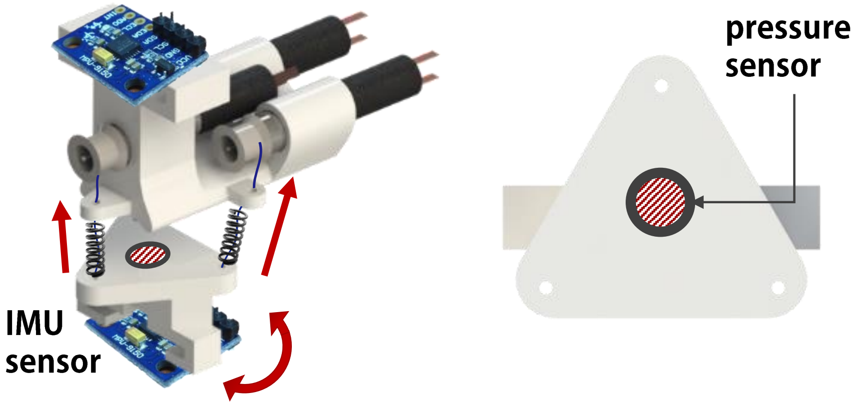

FIGURE 2.6: 3-DoF cutaneous haptic device design. The device is composed of two main parts: body and contact plate, which are connected by three wires actuated by three motors.

expected to perceive elaborate contact information, which will also allow more detailed grasping tasks, since stable grasping could be a difficult mission without complete haptic cue. This 3-DoF device supplements the contact perception of fingertip moving back and forth compared to the previous 2-DoF device, while it still contains the normal and shear (left and right) force feedback.

The 3-DoF cutaneous haptic device in Fig. 2.5 consists of two parts; 1) body part and 2) contact plate part, which basically adopted the design idea from [15]. Body part includes three micro DC motors (Faulhaber® DC motor, $\phi = 6$mm, $0.11W$, $64 : 1$ gear ratio). Small pulley is assembled with each motor shaft and fishing wire is wound on a pulley. Those wires are then connected to the vertices of triangle-shaped contact plate part. Wires are routed by small springs ($\phi =$ 3mm, 0.2N/mm) to provide resilence of contact plate. In the center of contact plate, piezoresistive force sensor (Interlink Electronics® 400 FSR) is attached to measure the magnitude of normal contact force. IMU sensors (Invensense® MPU-9150) are also attached to body and contact plate parts respectively, to measure the rotation of contact plate part w.r.t. body part. Equipped on user's finger, by controlling each motor properly, 3-DoF contact force can be generated onto fingertip for contact sensation. We utilize Arduino® UNO microcontroller board to receive the sensor data and send motor PWM values, using USB serial communication. The total weight and dimensions are 23g and $27 \times 48 \times 30\text{mm}^3$, excluding power supply and cables. Maximum normal contact force is about 1N, and 3-D contact force with roll/pitch range of about 20° can be provided to user's fingertip.

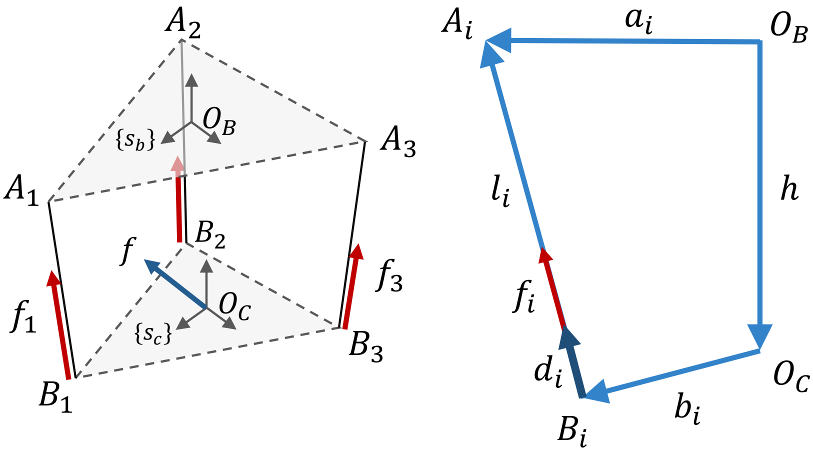

FIGURE 2.7: 3-DoF cutaneous haptic device scheme.

2.2.2 Control Design

For 3-DoF cutaneous device control, we want the desired force f^d to be transmitted onto user's fingertip. Using FSR force sensor and IMU sensor measurements, our control inputs $u = [u_1\ u_2\ u_3]^T \in \Re^3$, tensile forces exerted by each motor torque, are determined by device geometry and 2^{nd} order fingertip stiffness model [39]. The main geometrical parameters are represented in Fig. 2.7. A_1, A_2, and A_3 are vertices of fixed device body where motor torques are given, while B_1, B_2 and, B_3 are vertices of mobile contact plate where cable and plate are connected.

Our control objective is to make user's fingertip contact force f to be the desired force f^d with proper u.

$$f \to f^d \tag{2.1}$$

Then, f is assumed to be the same as $f_{plate} \in \Re^3$, the force exerted to contact plate by motor torques, since fingertip will be constantly contacting with the plate:

$$f \simeq f_{plate} \tag{2.2}$$

From device design,

$$f_{plate} = \begin{bmatrix} d_1 & d_2 & d_3 \end{bmatrix} \begin{bmatrix} f_1 \\ f_2 \\ f_3 \end{bmatrix} \tag{2.3}$$

where $d_i \in \Re^3$ is the unit vector of each wire's direction and $f_i \in \Re$ is the force exerted on vertex of contact plate, both seen in body frame $\{s_b\}$ and $i = 1, 2, 3$. Here, d_i is a normalized vector of $l_i \in \Re^3$ where

$$l_i = a_i - (Rb_i + h) \tag{2.4}$$

from geometry. Relative rotation matrix R can be calculated by two IMU sensors attached to body and contact plate. Height vector $h := [0\ 0\ \ -h_o + h_z]^T$ is determined by using FSR force sensor measurement, $f_{fsr} \in \Re$, and 2^{nd} order fingertip stiffness model [39],

$$f_{fsr} = k_f {h_z}^2 \tag{2.5}$$

where h_o is initial height (i.e., undeformed fingertip height), h_z is deformation in vertical direction and $k_f \in \Re$ is a stiffness model constant which can be various among people.

Since wires of the device are guided by springs,

$$f_i = u_i - kx_i \tag{2.6}$$

where $k \in \Re$ is a spring constant and $x_i \in \Re$ is a spring deformation of each wire which can be computed by R and b_i $(i = 1, 2, 3)$.

From using (2.3) to (2.6), contact force f of (2.2) can be determined as follows.

$$f = \begin{bmatrix} d_1 & d_2 & d_3 \end{bmatrix} \begin{bmatrix} f_1 \\ f_2 \\ f_3 \end{bmatrix} = G(u - kx) \tag{2.7}$$

By differentiating (2.7), contact force dynamics is obtained:

$$\dot{f} = G(\dot{u} - k\dot{x}) - \dot{G}(u - kx) \tag{2.8}$$

Here,

$$\dot{G} = \begin{bmatrix} \dot{d}_1 & \dot{d}_2 & \dot{d}_3 \end{bmatrix}$$

with time derivation of normalized vector:

$$\dot{d}_i = \frac{\dot{l}_i - d_i \|\dot{l}_i\|}{\|l_i\|}$$

where

$$\dot{l}_i = -(\dot{R}b_i + \dot{h}) = -(R[w]_\times b_i + \dot{h}) \tag{2.9}$$

To achieve our control objective (2.1) with contact force dynamics, we can define

$$(\dot{f} - \dot{f}^d) = -\lambda(f - f^d) \tag{2.10}$$

where $\lambda \in \Re$ is a positive constant. By combining (2.8) and (2.10),

$$\dot{f} = \dot{f}^d - \lambda(f - f^d) = G(\dot{u} - k\dot{x}) - \dot{G}(u - kx)$$

and finally,

$$\dot{u} = G^{-1}[\dot{f}^d - \lambda(f - f^d) - \dot{G}(u - kx)] + k\dot{x} \tag{2.11}$$

Then, control input u is obtained by simply integrating $\dot{u}$ and corresponding PWM value is computed for three motors to generate desired contact force. In practical, term $\dot{f}_d$ is ignored, with negligible quantity.

2.2.3 IMU Distortion Offset Calibration

In our control design, rotation matrix of contact plate R is measured in real-time by IMU sensors. However, magnetometer of IMU sensor is easily influenced by ferromagnetic materials, including motors. We utilize three motors which are small (ϕ = 6mm), but still influential in those IMU sensors. However, from some preliminary experiments to eliminate the distortion effect, we found that the distortion error from magnetometer is held constant with ignorable noise while relative position and orientation between motors and sensors are completely fixed.

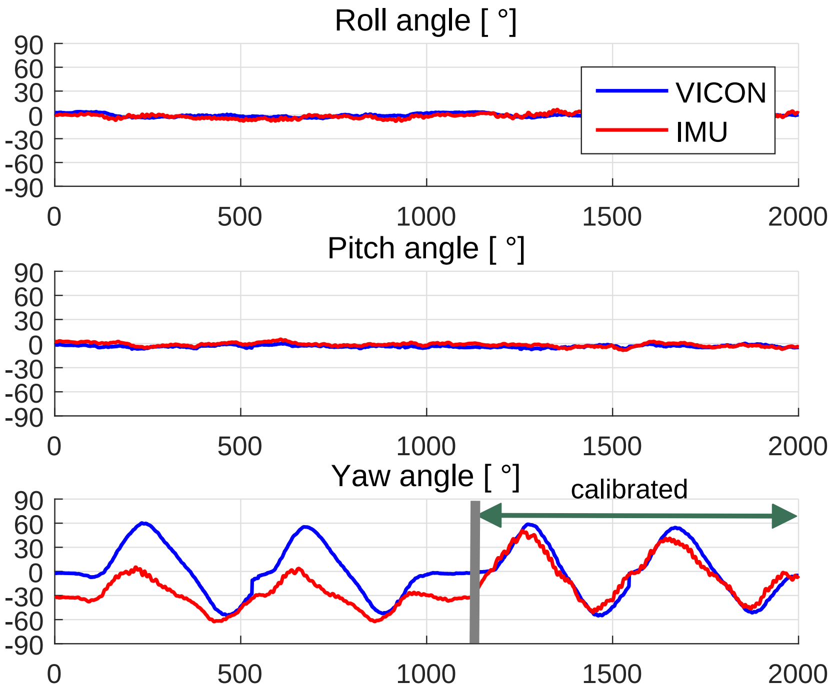

FIGURE 2.8: Result of magnetometer distortion calibration. When calibration applied to yaw rotation, RMS error of yaw angle decreased from 36.39° to 9.70°

To measure the magnetometer distortion offset $\Delta m \in \Re^3$ of two IMU sensors in Fig. 2.5, magnetometer values, $m_undistandm_dist \in \Re^3$ were measured in 10 different postures with 5 trials each ($N = 50$). Each value corresponds to undistorted (i.e., motors detached from device) and distorted (i.e., motors attached to device) magnetometer data, and we obtained the offset Δm by averaging them.

$$\Delta m = \frac{\Sigma_{i=1}^{10}(m_{dist,i} - m_{undist,i})}{N} \tag{2.12}$$

Then, simple experiment was performed to validate the magnetometer offset calibration. VICON® motion capture system was used to measure roll, pitch, and yaw angles of 3-DoF device for ground truth, and markers were attached to the device body. IMU sensor of device body (upper one) was chosen, and magnetometer calibration result was applied in the middle of the experiment. After manually rotating the device in three axis respectively, the result showed that, for roll and pitch rotations, there are no noticeable difference between two data, regardless of the calibration. Meanwhile, for yaw rotation as shown in Fig. 2.8, RMS errors of roll, pitch, and yaw angles between VICON and IMU sensor change from (3.22, 3.12, 36.39) to (2.62, 2.19, 9.70) [°].

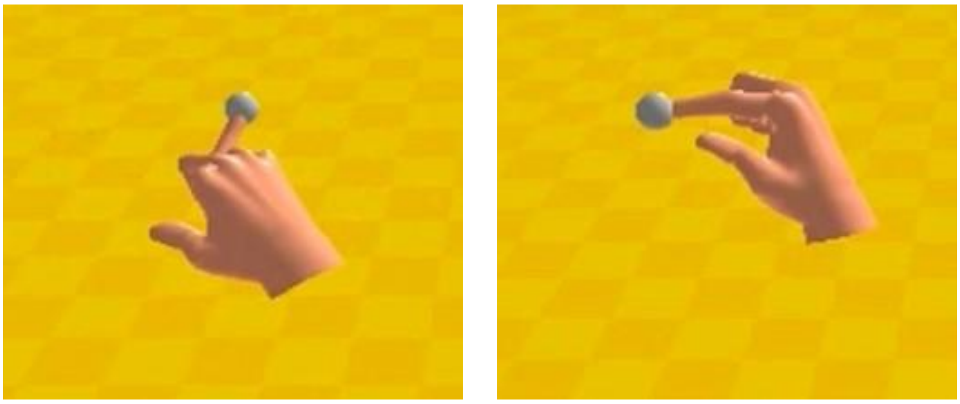

FIGURE 2.9: IMU on cutaneous device distorted by motors' ferromagnetism (left). IMU distortion calibrated (right).

Another validation of this result can be seen in Fig. 2.9, where this offset calibration is applied to our IMU-based 3-DoF cutaneous haptic device integrated with IMU-based hand tracking device, which will be discussed after.

2.2.4 Device Validation

To check the device design and control performance, experimental test was performed. Fig. 2.10 demonstrates the result of measured contact force when a step signal of reference force $f^d = 0.8$N was given. Reference (desired) contact force (dashed black) and contact force measured by FSR force sensor are shown in the figure. The result shows that the measured force reaches the reference force

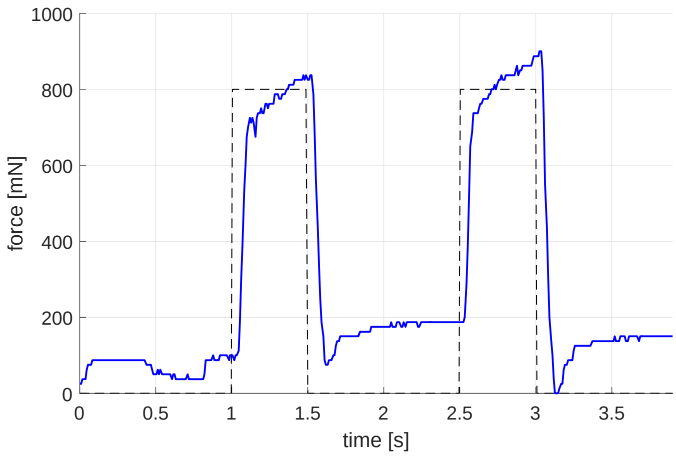

FIGURE 2.10: Step response of normal desired force for 3-DoF cutaneous haptic device. The dashed black line represents the reference force, and blue line represents the measured contact force from FSR sensor on contact plate. The rising time is about 0.2s.

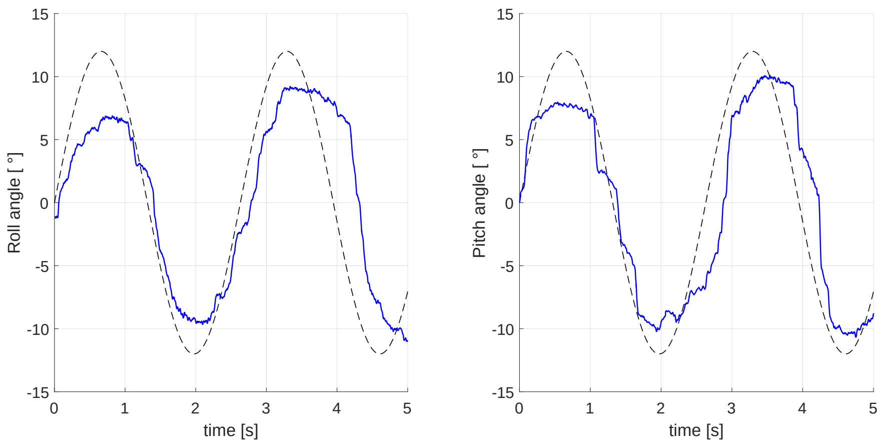

FIGURE 2.11: Sinusoidal response of roll and pitch angle for 3-DoF cutaneous haptic device. The dashed black line represents the reference angle given by corresponding (directional) sinusoidal reference force. The blue line represents the rotation angle from IMU sensors attached to the device.

with a rise time of about 0.2s. The sinusoidal reference forces were also given to check pitch and roll rotations. Due to fingertip compliances and IMU sensor noise, device and control performance for rotation seems to be improved, which will be including in future works.

2.2.5 Integration with Wearable Hand Tracking Interface

In order to utilize wearable cutaneous haptic device in virtual reality, precise localization of fingers and hand is necessary. Therefore, the 3-DoF cutaneous haptic device was integrated with IMU-based wearable hand tracking device introduced in [37]. This hand tracking device consists of 6 IMU sensors, which are also used for 3-DoF device, to measure the segment rotations of index finger and thumb. All readings of IMUs are sent to Arduino Nano® board with update rate of 200Hz. To rigidly attach the IMUs on the segments of the fingers while also improving user comfort, the sensors are attached to the ring-type parts with compliant structure using compression spring and slot as shown in Fig. 2.12.

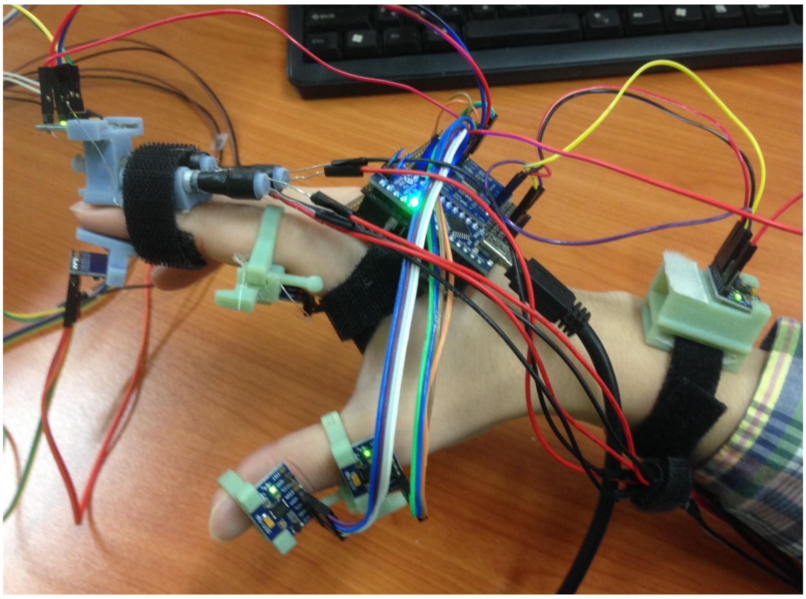

FIGURE 2.12: A 3-DoF cutaneous fingertip haptic device is integrated with our IMU-based hand tracking device. 6 IMU sensors of hand tracking device measure the rotations of finger segments for finger/hand localization.

While using this hand tracking interface, our 3-DoF cutaneous haptic device has advantage of using the same sensor; IMU sensor. Therefore, the integration of two devices has a range of possibilities in design, while fully exploiting the advantages of IMU sensors at the same time.

Preliminary test for integrated wearable haptic interface was proceeded (Fig. 2.13). User equipped the 3-DoF cutaneous haptic device on the index finger and the hand tracking device. Here, IMU sensor of hand tracking device for the middle phalanx is removed, while corresponding rotation data is measured by IMU sensor of cutaneous device body. IMU sensor of hand tracking device for the index finger was calibrated as mentioned in 2.2.3, as well as IMU sensors on cutaneous haptic device.

In virtual world, the virtual sphere and hand avatar are represented as shown in Fig. 2.13. User is able to see the bending motion of each finger, as his/her real fingers move with attached IMUs. While avatar's fingertip contacts with the virtual sphere, the contact force feedback is provided by equipped cutaneous device, which allows the user to perceive the stiffness and curvature of virtual sphere.

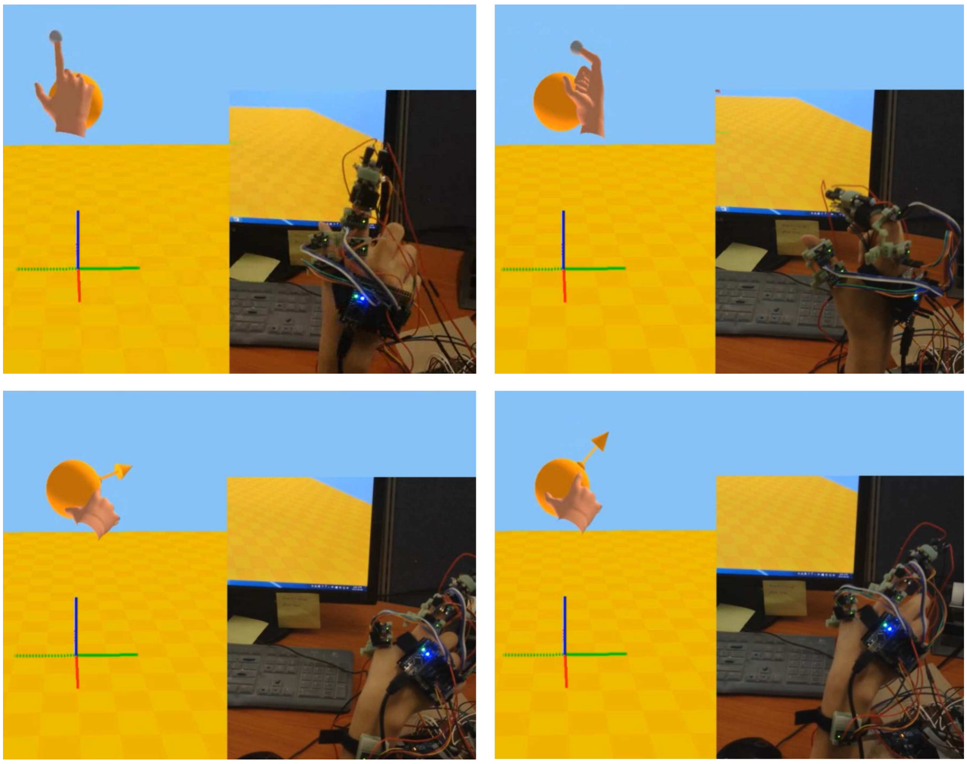

Figure 2.13: Preliminary experiment of the integrated wearable haptic interface; hand tracking device can capture any hand posture, while contact haptic feedback is given by 3-DoF cutaneous haptic device.

Chapter 3

Pseudo-Haptics with Cutaneous Haptic Feedback

3.1 Limitation of Cutaneous Haptic Device

Currently, cutaneous haptic devices are commonly used together with kinesthetic haptic devices such as Force Dimension's Omega®. This is because kinesthetic feedback generates the sense of touch through human musculoskeletal system which can provide relatively large haptic sensation compared to the cutaneous feedback. Accordingly, while utilizing our cutaneous haptic devices mentioned in Sec. 2, we found that the realism of the haptic sensation rapidly deteriorates after the contact due to the lack of kinesthetic feedback, which is basically supposed

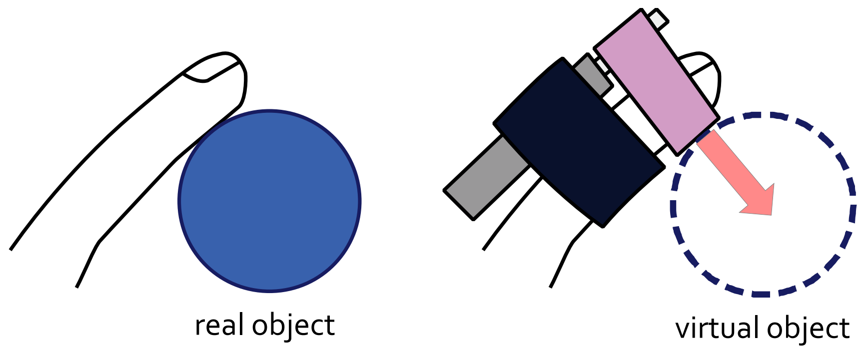

FIGURE 3.1: Human perception rapidly deteriorates due to the lack of kinesthetic haptic feedback, when solely using cutaneous haptic device.

to maintain the user's fingertip at the virtual object's boundary during contact [2]. Human user would feel awkward when the haptic feedback is provided while both fingertip avatar and actual fingertip penetrates the virtual object freely as shown in Fig. 3.1. This limitation of cutaneous haptic feedback will be permanent unless kinesthetic feedback is provided.

3.2 Application of Pseudo-Haptics Effect

In order to relieve these unrealistic experiences and partially substitute the absence of kinesthetic feedback, the concept of pseudo-haptics can be integrated with cutaneous haptic device. This illusionary feedback utilizes visual feedback and its dominance over haptic feedback, to present made-up haptic sensation without using additional physical haptic devices [28, 40]. Therefore, we explore a possible utility of pseudo-haptics for the cutaneous haptic device.

Natural approach of using this effect with cutaneous haptic device is to modify user's fingertip motion in virtual reality which is rendered to user, by regulating the C/D ratio [28]. When user's fingertip avatar contacts with the virtual object, we scale the fingertip's virtual displacement which is monitored on the computer screen, by

$$\Delta x_{\text{virtual}} = \alpha \cdot \Delta x_{\text{real}} \tag{3.1}$$

where $\alpha \in \Re$ defines the ratio of the virtual displacement $\Delta x_{\text{virtual}}$ seen on the screen to the user's real displacement Δx_{real}. This displacement modification is applied only when user contacts with virtual object's surface, which will also generate the contact force feedback via the equipped cutaneous haptic device with the computed desired force. Note that if $\alpha \leq 1$, a pseudo-haptics illusion of stiffer virtual object would arise as $\Delta x_{\text{virtual}}$ is scaled-down as compared to Δx_{real}, whereas if $\alpha \geq 1$, softer virtual object as $\Delta x_{\text{virtual}}$ scaled-up than Δx_{real}.

Chapter 4

Experimental Study

4.1 Experimental Settings

In [2], experimental study is examined for the possibility of integrating pseudo-haptics effect with cutaneous haptic device. As a first step of collaborating those two items, perceived stiffness of normal contact with a virtual plane when using our 2-DoF cutaneous haptic device (Fig. 2.1) was considered.

While using the 2-DoF cutaneous haptic device, human fingertip is represented as a 3D sphere in 3D virtual environment, displayed on the computer screen (Fig. 4.1). Then, the desired fingertip force $f_{des} \in \Re$, which will be generated during contact with virtual planes, is computed by

$$f_{des} = K_o \cdot \Delta x \quad \text{where} \quad K_o := \frac{\text{certain max. device force}}{\text{diameter of sphere}} \tag{4.1}$$

where $K_o \in \Re$ is the baseline stiffness of the virtual object's surface and $\Delta x \in \Re$ is the largest difference between the surface and fingertip sphere surface. Therefore, when the avatar sphere's penetration depth is the same as its diameter, the maximum fingertip force is attained. The corresponding desired motor angle is then obtained by referring to the calibration curve in Fig. 2.3. To measure the fingertip position during experiments, we use the VICON® motion capture system with markers attached on the device.

As shown in Fig. 4.1, subjects performed every trial in front of the computer screen while equipped with 2-DoF cutaneous haptic device on their index finger. Four VICON® motion capture cameras surrounded the subject in the distance of about 1m. The distance between the subject and the monitor screen was set to 1m. Subjects were able to see their fingers, yet, encouraged to focus on the fingertip sphere of the screen. There was no motor noise masking, also.

We construct the virtual 3D environment on the computer screen, consisting of a sphere, which represents the user's fingertip position, and two virtual planes divided in half by colors as shown in Fig. 4.2. Colors of the planes are switched for each trial of the experiment to reduce the sensory difference induced by different colors. These planes are located parallel to the ground surface with the same height.

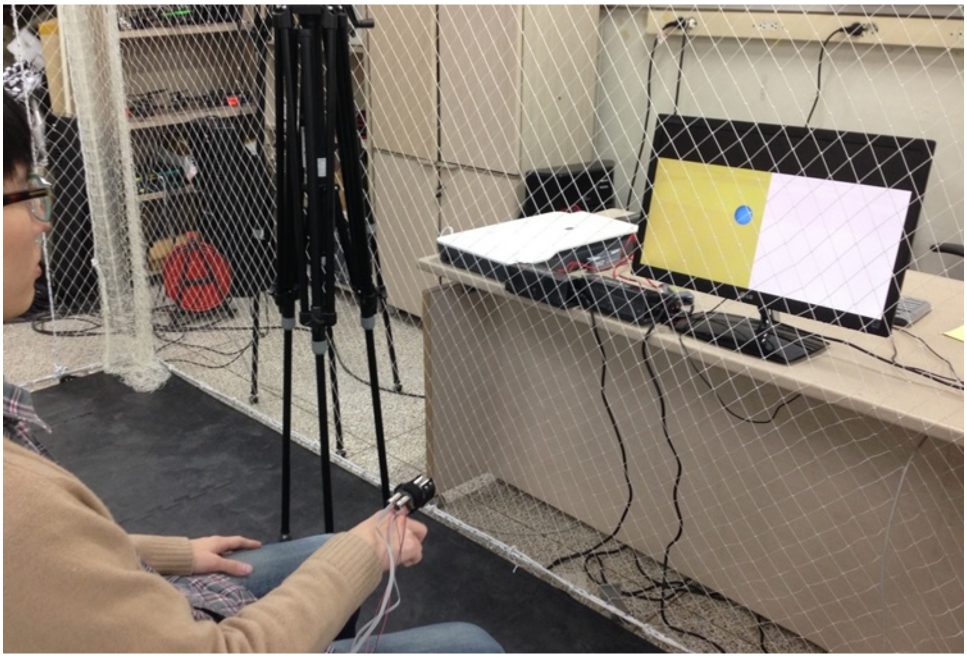

FIGURE 4.1: Environmental scene.

Cutaneous haptic feedback to the user is produced by the relation as given in (4.1) with $\Delta x = \Delta x_{\text{real}}$ (for Experiments #1 and #2: see below) or $\Delta x = \Delta x_{\text{virtual}}$ (for Experiment #3: see below), only when the fingertip sphere makes a contact with the planes. No haptic feedback is produced when the sphere loses the contact. The pseudo-haptics effect is simultaneously implemented by regulating α according to (3.1), also only when the fingertip sphere contacts with the planes. This pseudo-haptics effect is implemented only for the right plane in Fig. 4.2, which we call *PH-plane* (pseudo-haptics plane), with randomly varying α depending on the experiment trial. The left plane, which we call *RF-plane* (reference plane), has

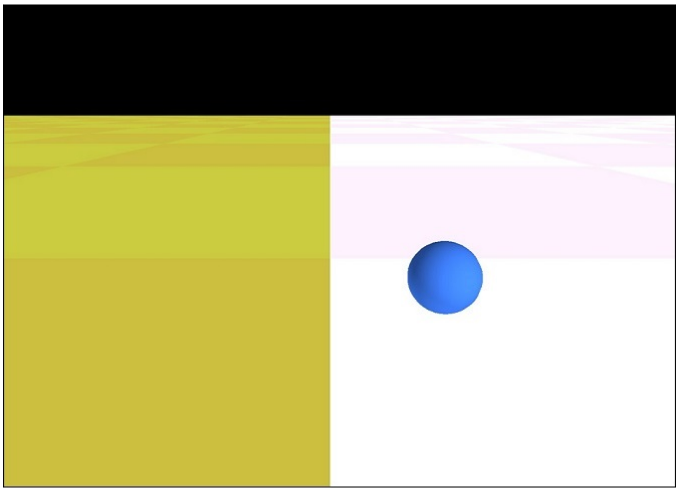

FIGURE 4.2: Virtual 3D environment with fingertip sphere, reference plane (RF-plane) without pseudo-haptics effect, and pseudo-haptics plane (PH-plane) with pseudo-haptics effect applied (right).

no pseudo-haptics effect with $\alpha \equiv 1$ throughout the whole experiment.

Human subject can freely move the fingertip sphere in the virtual world, by moving their real fingertip (i.e., finger or hand). However, when its penetrating displacement Δx exceeds certain threshold value during the contact, the cutaneous device force can be saturated. This force saturation can harm the stiffness perception, e.g., making users misperceive the object less stiff when the device force is saturated. To avoid this issue, at the moment of force saturation (detected by displacement measurement), we turned the color of the virtual plane, where the force saturation occurred, to red to notify the subject of this saturation. We also guided them before the experiment to avoid such saturation as much as possible.

Three Experiments, #1, #2 and #3, were performed separately with five human subjects, all male, from the age of 23 to 31, with no known perception disorder. All the subjects were right-handed and used their index finger of dominant hand for all the experiments. The experiments were conducted in accordance with the requirements of the Helsinki Declaration.

4.2 Experiment #1

The purpose of Experiment #1 is to investigate if the pseudo-haptics effect, when combined with the cutaneous feedback, can generate an illusionary perception of stiffer or softer virtual planes, as compared to the case of the sole usage of the cutaneous feedback without modifying visual cue. To achieve this, we set $\alpha = 1$ for the RF-plane through the Experiment #1, whereas randomly varying α from 0.2 to 1.6 with 0.2 interval was applied to PH-plane.

Each subject was allowed to spend enough time to get familiar with the device and environment first. After that, they were asked to carry out the classical Two Alternative Forced Choices (2AFC) with those two planes. They were instructed to contact with two virtual planes, and then to answer which was perceived stiffer between RF-plane and PH-plane, with randomly chosen α applied to the PH-plane. Three trials were given for each α, making 24 trials for each subject, and 120 trials totally.

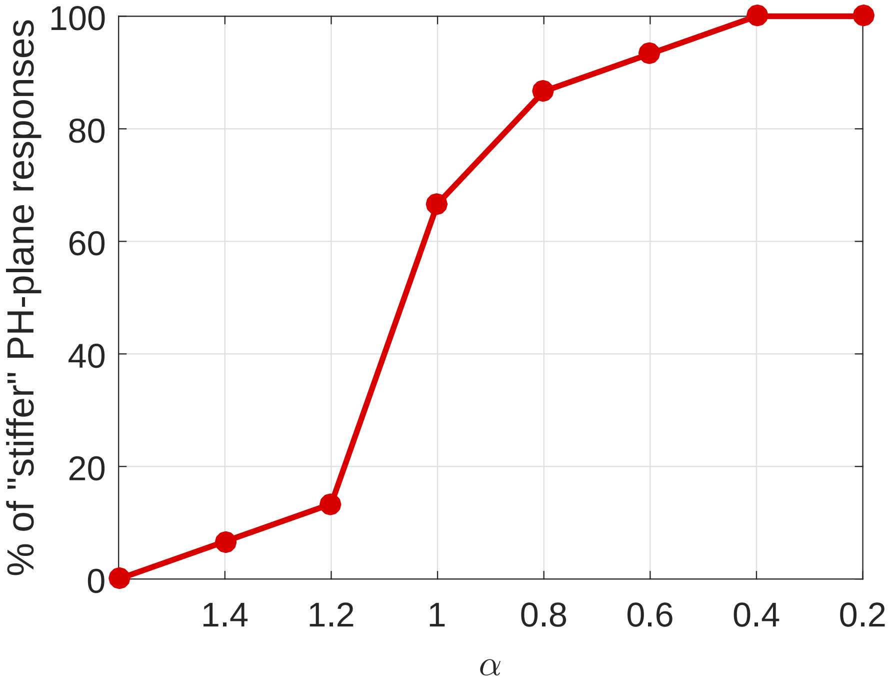

FIGURE 4.3: Result of Experiment #1: modulation of perceived virtual stiffness via pseudo-haptics effect α.

From Fig. 4.3, it is noticeable that pseudo-haptic feedback is indeed effective in rendering the virtual stiffness by sole manipulation of visual cue α. The y-axis value in Fig. 4.3 is the percentage of responses choosing PH-plane as the stiffer plane. Ideally, fifty percent of y-axis value means that the subjects reported that both planes rendered the similar (perceived) stiffness on average. When $\alpha < 1$, subjects tended to choose the PH-plane as the stiffer one, when $\alpha > 1$, exactly opposite situation occurred, i.e., RF-plane felt softer. This obviously displays the efficacy of pseudo-haptic feedback for our cutaneous haptic device, as it deceived subjects perceive as if the virtual plane became stiffer (with $\alpha < 1$) or softer (with $\alpha > 1$) depending on the visual cue α (C/D ratio).

4.3 Experiment #2

In Experiment #2, a quantitative analysis was examined on the effectiveness of the pseudo-haptics when integrated with the cutaneous feedback. We adjusted the stiffness K of the RF-plane with no pseudo-haptics effect applied (i.e., $\alpha = 1$) and compared it with the PH-plane with the fixed baseline stiffness K_o and randomized α.

More precisely, we randomly chose a certain α from 0.2 to 1.2 with 0.2 step-size and applied it to the PH-plane, which was haptically rendered via (4.1) with the baseline stiffness K_o. On the other hand, for the RF-plane with $\alpha = 1$ fixed, we gradually adjusted its stiffness K and applied it instead of the baseline K_o for (4.1). For each trial of Experiment #2, we increased or decreased K within the range of 0.2 to 5.0 with the interval of 0.2 while K_o fixed.

At each trial, the subjects were asked to perform the same operation of 2AFC as stated in Experiment #1 to tell which plane was perceived stiffer. For each set of (α, varying K), each subject had 4 trials, 2 with the increasing K and 2 with the decreasing K. We measured the value K when the subject's answer on which plane was stiffer changed, divided them by K_o, and averaged them from the 4

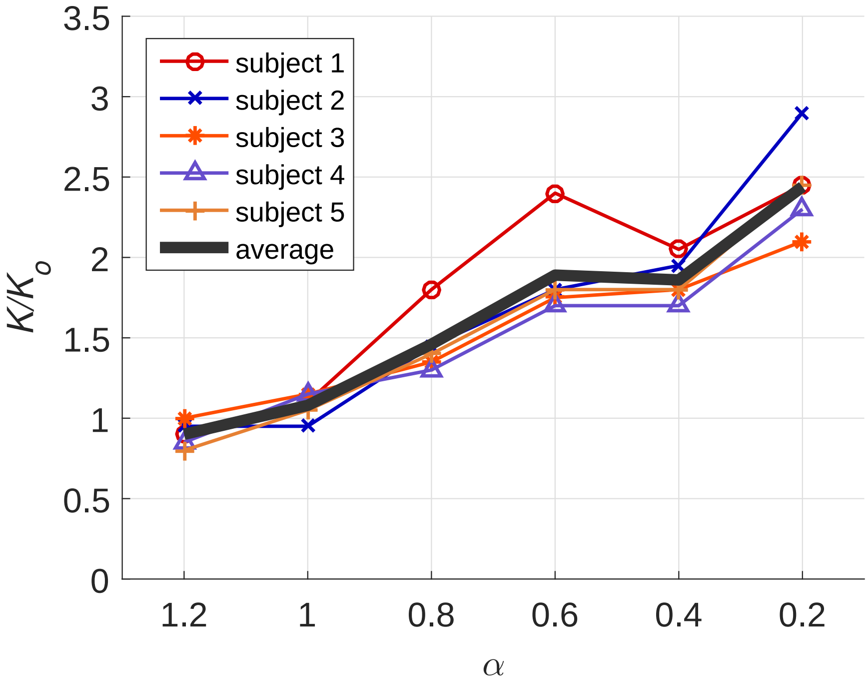

FIGURE 4.4: Result of Experiment #2: expansion of the renderable range of the perceived virtual stiffness via pseudo-haptics effect α.

trials. Then we used this averaged value of four K/K_o as the "representative" perceived stiffness value of the PH-plane with the pseudo-haptics effect.

The result of Experiment #2 is summarized in Fig. 4.4, where the y-axis represents the averaged value of K/K_o as defined above, which we used to denote "representative" stiffness of the PH-plane with the pseudo-haptics effect. Note that this result in Fig. 4.4 quantitatively characterizes the efficacy of the pseudo-haptics effect for our cutaneous haptic device in interacting with the virtual plane.

In other words, as can be seen from Fig. 4.4, pseudo-haptics effect for our 2-DoF cutaneous haptic device can render virtual plane at least twice stiffer than the case of utilizing cutaneous feedback only. It means that cutaneous haptic device of the motors with a half of current motor torque can achieve similar haptic perception when combined with pseudo-haptics effect. Since one of our motivation is to challenge with the limited stiffness level of cutaneous device due to the lack of kinesthetic feedback, utilizing a wider range of stiffness by means of pseudo-haptics seems possible to improve the limited device performance.

4.4 Experiment #3

In Experiment #3, which was a sort of optional experiment, we intentionally provided human subjects with contradictory haptic and visual cues (i.e., haptic feedback intending stiff perception while soft perception intention with visual feedback), to emphasize the importance/effectiveness of handling the pseudo-haptics effect for the cutaneous feedback device. For this, when computing cutaneous feedback, Δx in (4.1) was replaced by $\Delta x_{virtual}$ from (3.1), instead of Δx_{real} which was used in Experiment #1 and #2. By this modification, for instance, with $\alpha > 1$ (or $\alpha < 1$, resp.), the visual cue will suggest the virtual plane be softer (or stiffer, resp.) as the movement perceived visually is exaggerated (or mitigated, resp.) via (3.1). Yet, the haptic cue will suggest the same virtual plane

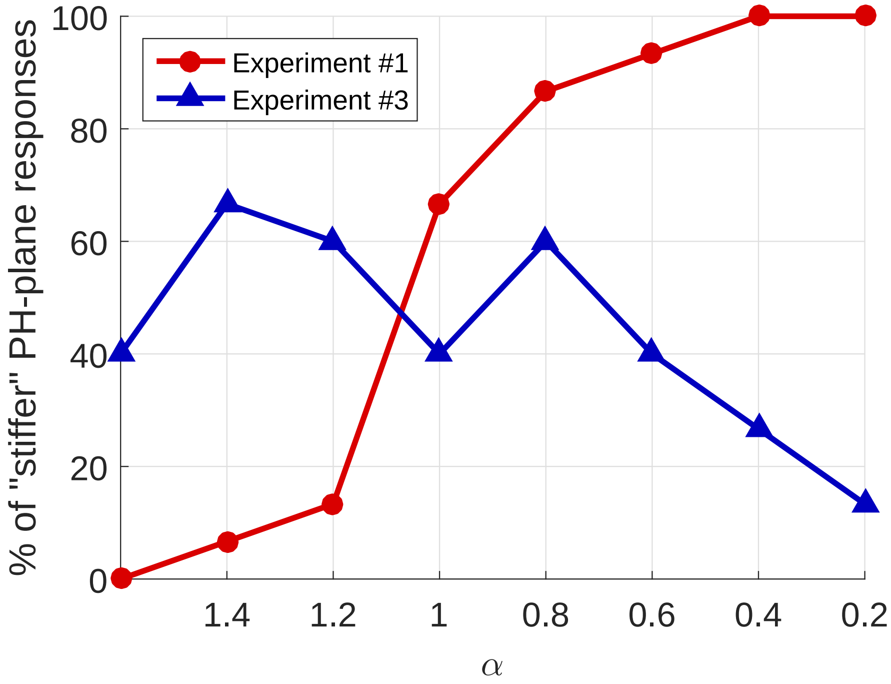

FIGURE 4.5: Result of Experiment #3: confusion induced by contradictory haptic and visual cues.

be stiffer (or softer, resp.) as the force is generated by the scaled-up (or scaled-down, resp.) displacement $\Delta x_{virtual} = \alpha \Delta x_{real}$. Other than this, way of choosing Δx, the subjects were asked to practice the same operation as Experiment #1 with all the other conditions to be the same.

The results are shown in Fig. 4.5, from which we can see that the subjects' responses are very different from that from Experiment #1. This inconsistency happened in almost every range of α. Both stiff and compliant sensation intended by pseudo-haptics effect are missing, with displaying no tendency. This, we believe, is the result of contrary visual and haptic cues. If $\alpha > 1$ (or $\alpha < 1$, resp.), the visual cue suggests softer plane (or stiffer, resp.), while the haptics cue suggests otherwise. For instance, 0.2 in α means that the subjects needed to move the actual fingertip position 5 times in PH-plane as much as in RF-plane to perceive same physical force in both planes. In other words, the same magnitude of subjects' real displacement Δx_{real} induced less force feedback in PH-plane compared to that in RF-plane. On the contrary, the fingertip sphere visualized on the screen will hardly move (stiffer motion) in PH-plane. In spite of the general belief that visual feedback is dominant over haptic feedback, subjects showed the opposite or irrelevant result; only 13 percent of the subjects answered that PH-plane was perceived stiffer.

4.5 Discussion

According to the results of the experiments above, pseudo-haptic feedback seems to assist human subjects to obtain better haptic sense of stiffness with our cutaneous feedback device in the situation of touching a virtual plane. As pseudo-haptic feedback modulated the virtual stiffness of the plane, subjects responded correspondingly. When $\alpha < 1$, the visual displacement on the screen became shortened in comparison with users' actual displacement, which deceived subjects into recognizing the virtual plane stiffer, and vice versa.

The effectiveness of pseudo-haptics with cutaneous haptic device was evaluated in Experiment #1, with its quantitative analysis in Experiment #2. From the results, the implementation of pseudo-haptics effect is expected to expand the stiffness perception to around 2 times in certain cases. Accordingly, a wider range of the stiffness perception becomes possible by modulating pseudo-haptics effect with stiffness K_o fixed.

Some interesting results were also observed when contradictory information of visual and haptic feedback was presented. In Experiment #3, $\Delta x_{virtual}$ was used as Δx to compute the desired force in (4.1), instead of previously used Δx_{real}. Unlike the results of Experiment #1 and #2, subjects generally responded that PH-plane felt softer in the range of $\alpha < 1$, where pseudo-haptic feedback was designed to generate stiffer sensation. At the same time, cutaneous haptic feedback in PH-plane delivered more compliant sensation in contrast with the pseudo-haptics. This indicates that although pseudo-haptic feedback uses its visual perception dominance over haptic feedback, that phenomenon is valid only for certain range of pseudo-haptics effect. Therefore, it would be more practical to utilize the pseudo-haptics as a complement for cutaneous haptic feedback, than totally rely on pseudo-haptics effect.

Chapter 5

Conclusion and Future Work

5.1 Conclusion

In this thesis, we present a novel design of cutaneous fingertip haptic device and examine the integration of cutaneous feedback device and pseudo-haptic feedback. 2-DoF cutaneous haptic device is developed using angle-force calibration result and applied to various haptic tasks. Development of design and control for 3-DoF cutaneous haptic device using IMU and FSR force sensors is proceeded for more accurate grasping. This 3-DoF device is also integrated with our IMU-based hand tracking device. To partially reduce the limitation of cutaneous haptic device, we perform experiments to show the efficacy of the pseudo-haptics when used for cutaneous fingertip haptic device. Case of contact with normal plane while using 2-DoF device is investigated, and the result indicates a possible way of utilizing pseudo-haptics and cutaneous haptic device.

5.2 Future Work

Future work includes the improvement of 3-DoF cutaneous haptic device and its application. By efficiently decreasing noise from IMU and FSR sensors, device performance is expected to improve with more accurate contact force provided. Modification of device design or sensors can also be considered for prominent wearability and portability as our motivation. Experiments of grasping tasks using the cutaneous haptic device integrated with the hand tracking device will be proceeded for the complete wearable haptic interface. Human study of pseudo-haptics with cutaneous haptic device will be extended to the fingertip stiffness perception of directional forces (i.e., left-right and back-and-forth).

Bibliography

[1] Inyoung Jang and Dongjun Lee. Experiments with cutaneous haptic feedback - a preliminary study. In *URAI*, pages 232–233, 2013.

[2] Inyoung Jang and Dongjun Lee. On utilizing pseudo-haptics for cutaneous fingertip haptic device. In *Haptics Symposium (HAPTICS), 2014 IEEE*, pages 635–639. IEEE, 2014.

[3] Mark Salada, J Edward Colgate, MV Lee, and Peter Vishton. Fingertip haptics: A novel direction in haptic display. In *Proceedings of the 8th mechatronics forum international conference*, pages 1211–1220, 2002.

[4] Kouta Minamizawa, Souichiro Fukamachi, Hiroyuki Kajimoto, Naoki Kawakami, and Susumu Tachi. Gravity grabber: wearable haptic display to present virtual mass sensation. In *ACM SIGGRAPH 2007 emerging technologies*, page 8. ACM, 2007.

[5] Domenico Prattichizzo, Francesco Chinello, Claudio Pacchierotti, and Kouta Minamizawa. Remotouch: A system for remote touch experience. In *RO-MAN, 2010 IEEE*, pages 676–679. IEEE, 2010.

[6] Claudio Pacchierotti, Francesco Chinello, Monica Malvezzi, Leonardo Meli, and Domenico Prattichizzo. Two finger grasping simulation with cutaneous and kinesthetic force feedback. In *Haptics: Perception, Devices, Mobility, and Communication*, pages 373–382. Springer, 2012.

[7] Nikolaos G Tsagarakis, T Horne, and Darwin G Caldwell. Slip aestheasis: A portable 2d slip/skin stretch display for the fingertip. In *Eurohaptics Conference, 2005 and Symposium on Haptic Interfaces for Virtual Environment and Teleoperator Systems, 2005. World Haptics 2005. First Joint*, pages 214–219. IEEE, 2005.

[8] Massimiliano Solazzi, Antonio Frisoli, and Massimo Bergamasco. Design of a cutaneous fingertip display for improving haptic exploration of virtual objects. In *RO-MAN, 2010 IEEE*, pages 1–6. IEEE, 2010.

[9] Brian T Gleeson, Scott K Horschel, and William R Provancher. Design of a fingertip-mounted tactile display with tangential skin displacement feedback. *Haptics, IEEE Transactions on*, 3(4):297–301, 2010.

[10] Kouta Minamizawa, Domenico Prattichizzo, and Susumu Tachi. Simplified design of haptic display by extending one-point kinesthetic feedback to multipoint tactile feedback. In *Haptics Symposium, 2010 IEEE*, pages 257–260. IEEE, 2010.

[11] Kouta Minamizawa, Koichi Tojo, Hiroyuki Kajimoto, Naoki Kawakami, and Susumu Tachi. Haptic interface for middle phalanx using dual motors. In *Proceedings of the EuroHaptics 2006 Conference*, pages 235–240, 2006.

[12] Charith Lasantha Fernando, Masahiro Furukawa, Tadatoshi Kurogi, Kyo Hirota, Sho Kamuro, Katsunari Sato, Kouta Minamizawa, and Susumu Tachi. Telesar v: Telexistence surrogate anthropomorphic robot. In *ACM SIGGRAPH 2012 Emerging Technologies*, page 23. ACM, 2012.

[13] Massimiliano Solazzi, Antonio Frisoli, and Massimo Bergamasco. Design of a novel finger haptic interface for contact and orientation display. In *Haptics Symposium, 2010 IEEE*, pages 129–132. IEEE, 2010.

[14] Francesco Chinello, Monica Malvezzi, Claudio Pacchierotti, and Domenico Prattichizzo. A three dofs wearable tactile display for exploration and manipulation of virtual objects. In *Haptics Symposium (HAPTICS), 2012 IEEE*, pages 71–76. IEEE, 2012.

[15] Domenico Prattichizzo, Francesco Chinello, Claudio Pacchierotti, and Monica Malvezzi. Towards wearability in fingertip haptics: a 3-dof wearable device for cutaneous force feedback. *Haptics, IEEE Transactions on*, 6(4): 506–516, 2013.

[16] Francesco Chinello, Monica Malvezzi, Claudio Pacchierotti, and Domenico Prattichizzo. Design and development of a 3rrs wearable fingertip cutaneous device. In *Advanced Intelligent Mechatronics (AIM), 2015 IEEE International Conference on*, pages 293–298. IEEE, 2015.

[17] Daniele Leonardis, Massimiliano Solazzi, Ilaria Bortone, and Antonio Frisoli. A wearable fingertip haptic device with 3 dof asymmetric 3-rsr kinematics. In *World Haptics Conference (WHC), 2015 IEEE*, pages 388–393. IEEE, 2015.

[18] Zhan Fan Quek, Samuel Schorr, Ilana Nisky, William Provancher, and Allison M Okamura. Sensory substitution using 3-degree-of-freedom tangential and normal skin deformation feedback. In *Haptics Symposium (HAPTICS), 2014 IEEE*, pages 27–33. IEEE, 2014.

[19] Alvaro G Perez, Daniel Lobo, Francesco Chinello, Gabriel Cirio, Monica Malvezzi, Jose San Martin, Domenico Prattichizzo, and Miguel A Otaduy. Soft finger tactile rendering for wearable haptics. In *World Haptics Conference (WHC), 2015 IEEE*, pages 327–332. IEEE, 2015.

[20] Stefano Scheggi, Leonardo Meli, Claudio Pacchierotti, and Domenico Prattichizzo. Touch the virtual reality: using the leap motion controller for hand tracking and wearable tactile devices for immersive haptic rendering. In *ACM SIGGRAPH 2015 Posters*, page 31. ACM, 2015.

[21] Tommaso Lisini Baldi, Mostafa Mohammadi, Stefano Scheggi, and Domenico Prattichizzo. Using inertial and magnetic sensors for hand tracking and rendering in wearable haptics. In *World Haptics Conference (WHC), 2015 IEEE*, pages 381–387. IEEE, 2015.

[22] Leonardo Meli, Stefano Scheggi, Claudio Pacchierotti, and Domenico Prattichizzo. Wearable haptics and hand tracking via an rgb-d camera for immersive tactile experiences. In *ACM SIGGRAPH 2014 Posters*, page 56. ACM, 2014.

[23] Domenico Prattichizzo, Claudio Pacchierotti, and Giulio Rosati. Cutaneous force feedback as a sensory subtraction technique in haptics. *Haptics, IEEE Transactions on*, 5(4):289–300, 2012.

[24] Domenico Prattichizzo, Claudio Pacchierotti, Stefano Cenci, Kouta Minamizawa, and Giulio Rosati. Using a fingertip tactile device to substitute kinesthetic feedback in haptic interaction. In *Haptics: Generating and Perceiving Tangible Sensations*, pages 125–130. Springer, 2010.

[25] Asad Tirmizi, Claudio Pacchierotti, and Domenico Prattichizzo. On the role of cutaneous force in teleoperation: subtracting kinesthesia from complete haptic feedback. In *World Haptics Conference (WHC), 2013*, pages 371–376. IEEE, 2013.

[26] Samuel Schorr, Zhan Fan Quek, Robert Y Romano, Ilana Nisky, William Provancher, and Allison M Okamura. Sensory substitution via cutaneous skin stretch feedback. In *Robotics and Automation (ICRA), 2013 IEEE International Conference on*, pages 2341–2346. IEEE, 2013.

[27] Lonel Dominjon, Anatole Lécuyer, Jean-Marie Burkhardt, Paul Richard, and Simon Richir. Influence of control/display ratio on the perception of

mass of manipulated objects in virtual environments. In *Virtual Reality, 2005. Proceedings. VR 2005. IEEE*, pages 19–25. IEEE, 2005.

[28] Anatole Lecuyer, Sabine Coquillart, Abderrahmane Kheddar, Paul Richard, and Philippe Coiffet. Pseudo-haptic feedback: can isometric input devices simulate force feedback? In *Virtual Reality, 2000. Proceedings. IEEE*, pages 83–90. IEEE, 2000.

[29] Mandayam A Srinivasan, Gerald Lee Beauregard, and David L Brock. The impact of visual information on the haptic perception of stiffness in virtual environments. In *ASME Winter Annual Meeting*, volume 58, pages 555–559, 1996.

[30] Anatole Lécuyer, Jean-Marie Burkhardt, and Laurent Etienne. Feeling bumps and holes without a haptic interface: the perception of pseudo-haptic textures. In *Proceedings of the SIGCHI conference on Human factors in computing systems*, pages 239–246. ACM, 2004.

[31] Ferran Argelaguet, David Antonio Gómez Jáuregui, Maud Marchal, and Anatole Lécuyer. A novel approach for pseudo-haptic textures based on curvature information. In *Haptics: Perception, Devices, Mobility, and Communication*, pages 1–12. Springer, 2012.

[32] David Antonio Gomez Jauregui, Ferran Argelaguet, Anne-Helene Olivier, Maud Marchal, Franck Multon, and Anatole Lecuyer. Toward "pseudo-haptic avatars": Modifying the visual animation of self-avatar can simulate

the perception of weight lifting. *Visualization and Computer Graphics, IEEE Transactions on*, 20(4):654–661, 2014.

[33] Merwan Achibet, Maud Marchal, Ferran Argelaguet, and Anatole Lécuyer. The virtual mitten: A novel interaction paradigm for visuo-haptic manipulation of objects using grip force. In *3D User Interfaces (3DUI), 2014 IEEE Symposium on*, pages 59–66. IEEE, 2014.

[34] Min Li, Jelizaveta Konstantinova, Emanuele L Secco, Allen Jiang, Hongbin Liu, Thrishantha Nanayakkara, Lakmal D Seneviratne, Prokar Dasgupta, Kaspar Althoefer, and Helge A Wurdemann. Using visual cues to enhance haptic feedback for palpation on virtual model of soft tissue. *Medical & Biological Engineering & Computing*, pages 1–10, 2015.

[35] Taku Hachisu, Gabriel Cirio, Maud Marchal, Anatole Lécuyer, and Hiroyuki Kajimoto. Pseudo-haptic feedback augmented with visual and tactile vibrations. In *VR Innovation (ISVRI), 2011 IEEE International Symposium on*, pages 327–328. IEEE, 2011.

[36] Taku Hachisu, Gabriel Cirio, Maud Marchal, Anatole Lécuyer, and Hiroyuki Kajimoto. Virtual chromatic percussions simulated by pseudo-haptic and vibrotactile feedback. In *Proceedings of the 8th International Conference on Advances in Computer Entertainment Technology*, page 20. ACM, 2011.

[37] Yongseok Lee, Inyoung Jang, and Dongjun Lee. Enlarging just noticeable differences of visual-proprioceptive conflict in vr using haptic feedback. In *World Haptics Conference (WHC), 2015 IEEE*, pages 19–24. IEEE, 2015.

[38] ChangSu Ha, Sangyul Park, Jongbeom Her, Inyoung Jang, Yongseok Lee, Gun Rae Cho, Hyoung Il Son, and Dongjun Lee. Whole-body multi-modal semi-autonomous teleoperation of mobile manipulator systems. In *Robotics and Automation (ICRA), 2015 IEEE International Conference on*, pages 164–170. IEEE, 2015.

[39] Kwi-Ho Park, Byoung-Ho Kim, and Shinichi Hirai. Development of a soft-fingertip and its modeling based on force distribution. In *Robotics and Automation, 2003. Proceedings. ICRA'03. IEEE International Conference on*, volume 3, pages 3169–3174. IEEE, 2003.

[40] Anatole Lécuyer. Simulating haptic feedback using vision: A survey of research and applications of pseudo-haptic feedback. *Presence: Teleoperators and Virtual Environments*, 18(1):39–53, 2009.

요약

본 논문에서는 손끝 햅틱 장비의 제작과 이를 위한 의사 햅틱의 활용에 대해서 기술한다. 사용자는 제안된 손끝 햅틱 장비를 손에 착용하여 가상 현실에서의 접촉감각을 느낄 수 있으며, 각각 2자유도와 3자유도의 접촉력을 전달하는 장비가 개발되었다. 2자유도 장비 구동을 위한 각도-힘 관계가 실험적으로 도출되었으며, 3자유도 손끝 햅틱 장비는 기존에 개발된 손 위치 추정 장비와 통합되어 착용형 햅틱 인터페이스의 가능성을 엿보았다. 이와 동시에 손끝 햅틱 장비의 물리적인 한계를 완화하기 위해 의사 햅틱의 개념을 적용하였으며, 가상 평면 접촉에 대한 실험이 진행되었다. 실험 결과, 의사 햅틱을 이용하여 사용자에게 전달되는 손끝접촉 감각을 조절할 수 있음을 밝혔으며, 기존에 손끝 장비가 전달하는 힘의 약 2배의 단단함을 줄 수 있음을 확인하였다.

주요어: Cutaneous haptic feedback, Wearable haptic device, Pseudo-haptics, Fingertip Perception, Multimodal
학번: *2013-20710*